

# Numerical Solution for the Nonlinear Schrodinger Equation

Divjyot Singh, Gonzalo Ferrandez Quinto

November 2023

Final project for ESAM 446 with Prof. Daniel Lecoanet  
Northwestern University

## 1 Introduction

Schrodinger's equation can be used to model a large number of varying physical systems. The non linear form can be used for optics, acoustics, plasma physics, hydrodynamics, and heat pulses in solids to name a few examples (Seadawy, 2012). The form of partial differential equation solved for this project is:

$$i\partial_t\Psi = -\frac{1}{2}\Delta\Psi + g\Psi|\Psi|^2, \quad \Psi(0, x) = \Psi_0(x), \quad (t, x) \in \mathbb{T} \times \mathbb{R}^2, \quad g \in \mathbb{R}, g \geq 0 \quad (1)$$

In this equation (Zakharov & Manakov, 1974), the time evolution of  $\Psi(t, x)$  is being solved.

This equation is also known as the Gross-Pitaevskii equation. It can be used to model bosonic condensed matter at low temperatures such as the Bose-Einstein condensate (Gross, 1961). At low temperatures, all bosons will be forced to occupy the same ground quantum state, therefore the wave-function  $\Psi$  is able to represent the quantum state of a single boson with the interpretation that  $|\Psi|^2$  is the probability density function. For  $N$  bosons, as all of them occupy the same energy state, the quantum state would be:

$$\Phi(t, x) = \prod_{i=1}^N \Psi(t, x) \quad (2)$$

where  $\Psi$  is the wave-function of a single boson.

The parameter  $g$ , would represent the strength of the interaction between bosons, in this case repulsive when  $g > 0$ . In the original equation, a trapping potential  $V(x)\Psi$  term is missing on the RHS of the equation, but for the purpose of this project, this potential is zero inside the domain and infinity everywhere else. This equals to stating that the wave-function  $\Psi$  satisfies Dirichlet boundary

condition equal to zero at the boundary. Therefore the trapped bosonic matter is confined to a 2-dimensional box with domain  $\Omega$  and boundary  $\partial\Omega$ .

$$\Psi(t, x) = 0 \quad \forall x \in \partial\Omega \quad (3)$$

## 2 Numerical Set up

For two spatial dimensions, the PDE can be rewritten as:

$$i\partial_t\Psi = -\frac{1}{2}(\partial_x^2 + \partial_y^2)\Psi + g\Psi|\Psi|^2 \quad (4)$$

The variable  $\Psi$  is treated as a complex variable. The equation can be treated as a diffusion reaction equation and use operator splitting. Hence, the equations can be split into the following terms:

$$M\partial_t\Psi + L\Psi = F(\Psi), \quad M = I, \quad L = -i\frac{1}{2}(\partial_x^2 + \partial_y^2), \quad F(\Psi) = -ig\Psi|\Psi|^2 \quad (5)$$

The equation 5 is solved using operator splitting. The terms in  $L$  are treated implicitly using the Crank-Nicolson scheme and the  $F(\Psi)$  term is treated explicitly using the RK22 scheme. The PDE is split into these operations:

$$\partial_t\Psi = -i\frac{1}{2}(\partial_x^2)\Psi \quad (6)$$

$$\partial_t\Psi = -i\frac{1}{2}(\partial_y^2)\Psi \quad (7)$$

$$\partial_t\Psi = -ig\Psi|\Psi|^2 \quad (8)$$

To ensure second order accuracy, time steps are taken in the following sequence:

$$D_x(\Delta t/2) \rightarrow D_y(\Delta t/2) \rightarrow R(\Delta t/2) \rightarrow R(\Delta t/2) \rightarrow D_y(\Delta t/2) \rightarrow D_x(\Delta t/2). \quad (9)$$

Here  $D_x$ ,  $D_y$ , and  $R$  represents the timesteppers for equations 6, 7, and 8 respectively.  $\Delta t/2$  in parenthesis represents that the timestepper was updated for a half time step. Hence, at every time step, each timestepper takes two half time steps, which is equivalent to one full timestep. A second order accurate timestepping scheme is used because it is a reasonably accurate and fast scheme used in the field.

The boundary conditions are applied inside the reaction timestepper by defining a BC function in the reaction timestepper. The BC function explicitly forces the wave function to be zero at the desired regions. In the diffusion term, the BC of the particle in a box are always applied implicitly by setting the initial and final diagonal terms of  $M$  to zero. The first and last row of  $L$  are also set to zero except the first and last diagonal terms, which are 1. This ensures the boundary conditions are met at every timestep. For the single-slit diffraction,

the additional barrier boundary conditions are specified only in the reaction term due to its complexity.

It should be noted that all algorithms used in the ESAM 446 class could be used for complex variables by changing all matrix data structures to complex form.

### 3 Testing the Algorithm

To test the algorithm, the case is reduced to a linear case by setting  $g = 0$ , which is equivalent to the linear case. By using a resolution of  $\Delta t = 0.025$ , the simulation gives the result as shown in Figure 1. Figure 1 **(a)** represents the solution at  $t = 5$  and Fig. 1 **(b)** represents the error with the analytic solution at the same time. At the final time  $t = 5$ , the results are compared with the analytical solution, which is given by equation:

$$\Psi(t, x, y) = \frac{1}{\sqrt{50}} \left[ \sin\left(\frac{\pi x}{10}\right) \sin\left(\frac{\pi y}{10}\right) e^{\frac{-it}{100}} + \sin\left(\frac{2\pi x}{5}\right) \sin\left(\frac{2\pi y}{5}\right) e^{\frac{-i16t}{100}} \right] \quad (10)$$

In Fig. 2, the error between the numerical solution and the analytical solution is plot. It can be seen that the error reduces as  $\frac{1}{\sqrt{50}} O(\Delta t^2)$  as the resolution increases, verifying the second order accuracy of our algorithm.

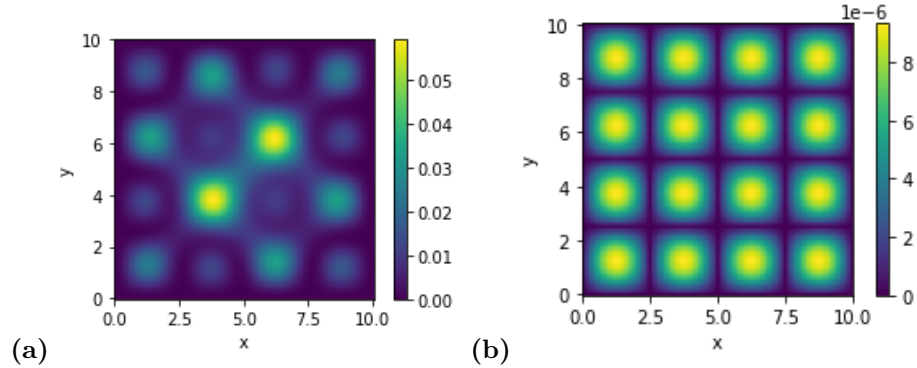


Figure 1: **(a)** This plot represents the absolute value squared of the final state at  $t=5$ , for initial conditions  $\Psi(t = 0, x, y) = \frac{1}{\sqrt{50}} \left[ \sin\left(\frac{\pi x}{10}\right) \sin\left(\frac{\pi y}{10}\right) + \sin\left(\frac{2\pi x}{5}\right) \sin\left(\frac{2\pi y}{5}\right) \right]$  **(b)** This plot represents the absolute value of the error between the simulation and the analytic solution at  $t=5$ .

### 4 Failed Attempt

The original PDE, equation 4, was first sought to be solved by splitting the real and imaginary parts of  $\Psi(t, x)$ , such that:

$$\Psi(t, x) = u_1(t, x) + iv_1(t, x). \quad (11)$$

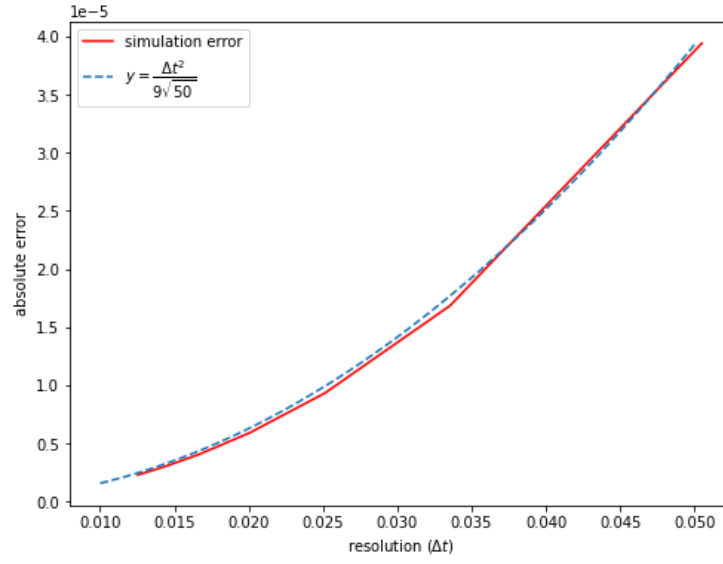


Figure 2: This figure depicts the maximum simulation error compared to the analytical solution for  $g = 0$  at different time stepping resolutions. It can be observed that the error is proportional to the square of the resolution. These simulations are run for 5 seconds with initial :  $\Psi(t = 0, x, y) = \frac{1}{\sqrt{50}}[\sin(\frac{\pi x}{10})\sin(\frac{\pi y}{10}) + \sin(\frac{2\pi x}{5})\sin(\frac{2\pi y}{5})]$

Plugging it in equation 4, the following equation is obtained

$$i\partial_t(u_1 + iv_1) = (\partial_x^2 + \partial_y^2)(u_1 + iv_1) + g(u_1 + iv_1)|(u_1 + iv_1)|^2. \quad (12)$$

By separating the real and imaginary parts, the following system of equations is obtained:

$$\partial_t v_1 = -\partial_x^2 u_1 - \partial_y^2 u_1 - g u_1 (u_1^2 + v_1^2) \quad (13)$$

$$\partial_t u_1 = \partial_x^2 v_1 + \partial_y^2 v_1 + g v_1 (u_1^2 + v_1^2) \quad (14)$$

The system of equations for  $u_1(x, t)$  and  $v_1(x, t)$  is solved by building a state vector with the two variables. Treating the equations as a diffusion-reaction equation system and use operator splitting. Hence, these equations can be split into the following 3 equations:

$$\partial_t \begin{bmatrix} u_1 \\ v_1 \end{bmatrix} = \begin{bmatrix} 0 & \partial_x^2 \\ -\partial_x^2 & 0 \end{bmatrix} \begin{bmatrix} u_1 \\ v_1 \end{bmatrix} \quad (15)$$

$$\partial_t \begin{bmatrix} u_1 \\ v_1 \end{bmatrix} = \begin{bmatrix} 0 & \partial_y^2 \\ -\partial_y^2 & 0 \end{bmatrix} \begin{bmatrix} u_1 \\ v_1 \end{bmatrix} \quad (16)$$

$$\partial_t \begin{bmatrix} u_1 \\ v_1 \end{bmatrix} = \begin{bmatrix} g v_1 (u_1^2 + v_1^2) \\ -g u_1 (u_1^2 + v_1^2) \end{bmatrix} \quad (17)$$

The equations 15 and 16 are solved implicitly using the Crank-Nicolson scheme and equation 17 explicitly using the RK22 scheme. To ensure second order accuracy, timesteps are taken as described in equation 9.

However, the solution using this blew up to infinity. This can be attributed to the instability of this scheme, due to the positive term on the RHS of equation 17 for  $u_1$  when  $g > 0$ , which makes this problem set up ill-posed. In this case, given some initial conditions, the solution would grow to infinity, making it an ineffective approach to solve the PDE. One could force solutions by taking extremely small time-steps and forcing a normalization condition for  $\Psi(t, x, y)$  such that its double integral in the domain equaled one. An attempt to normalize the wave function to one in the domain, however, did not lead to fruition, which further highlights why this is an ineffective approach. This is the reason the problem was solved with complex matrices instead.

## 5 Example Simulations

In this section, all the simulations will be solved in a 2D box with  $x, y \in (0, 10)$ . These simulations will represent interesting behaviours of the Non-Linear Schrodinger equation with different  $g$  values and inner boundary condition.

## 5.1 Linear Schrodinger Equation

The PDE of equation 4 is solved using the value of  $g = 0$  and initial conditions:

$$\Psi(t = 0, x, y) = \frac{1}{\sqrt{50}} [\sin(\frac{\pi x}{10}) \sin(\frac{\pi y}{10}) + \sin(\frac{2\pi x}{5}) \sin(\frac{2\pi y}{5})] \quad (18)$$

This initial condition is a normalized superposition of two eigenmodes of the linear Schrodinger equation solved in a square box boundary. This eigenmodes are the stationary solutions of the problem and have a value of 0 at the boundary. It can be seen in Fig. 4, how the solution is oscillating between two modes. This is the expected result as in the analytic solution, equation 10, the time evolution is given by a complex phase factor multiplying each eigenmode. Therefore the solution will be oscillating between two states due to the relative phase of the eigenmodes.

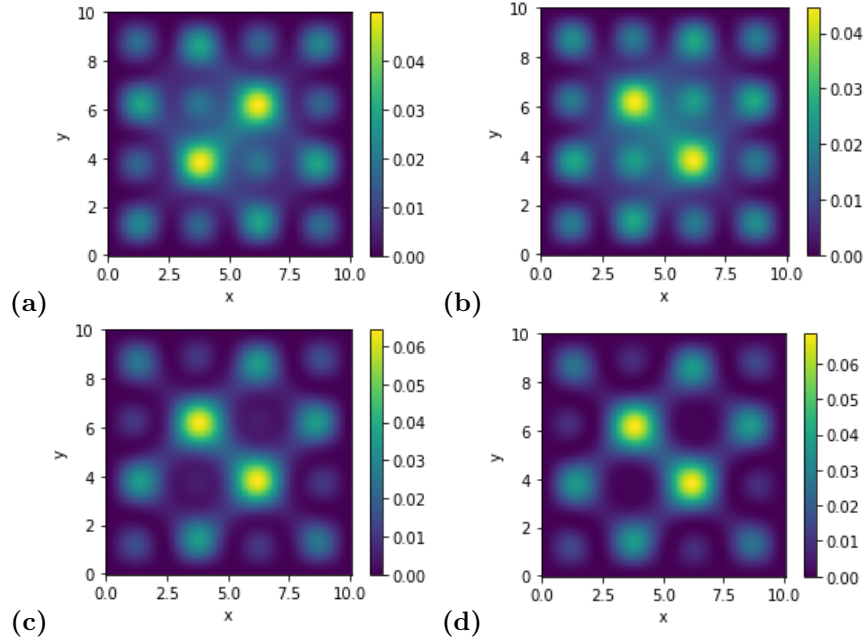


Figure 3: This figure represents the time evolution for the PDE of equation 4 using operator splitting. The value of  $|\Psi(t, x, y)|^2$  is being plotted, which represents a discrete probability density function. The time step is  $\Delta t = 0.025$ . The grid spacing is  $\Delta x = 0.05$ . The different plots represent the time evolution of the initial condition in equation 18 with the value of  $g = 0$ . (a)  $t = 1$  (b)  $t = 1.5$  (c)  $t = 2$  (d)  $t = 2.5$

## 5.2 Single Slit Diffraction

This is a special case of the linear Schrodinger equation where the boundary conditions are set such that the wave function is 0 at the central barriers, except at the center where there is a slit. The wave packet is able to go through this slit.

The initial conditions are a Gaussian wave packet such as:

$$\Psi(t = 0, x, y) = e^{-(x-1)^2} e^{-(y-5)^2} e^{8i\pi(x-1)} \quad (19)$$

In this initial condition, the Gaussian wave is centered around  $(x, y) = (1, 5)$  travelling to the right with wave number  $k_x = 8\pi$  and  $k_y = 0$ . This initial wave packet can be seen in Fig. 4 (a). In Figs. 4 (b) and 4 (c), it can be seen how the wave packet diffracts. Finally, in 4 (d), the characteristic wave diffraction pattern of a single slit can be seen on the right boundary.

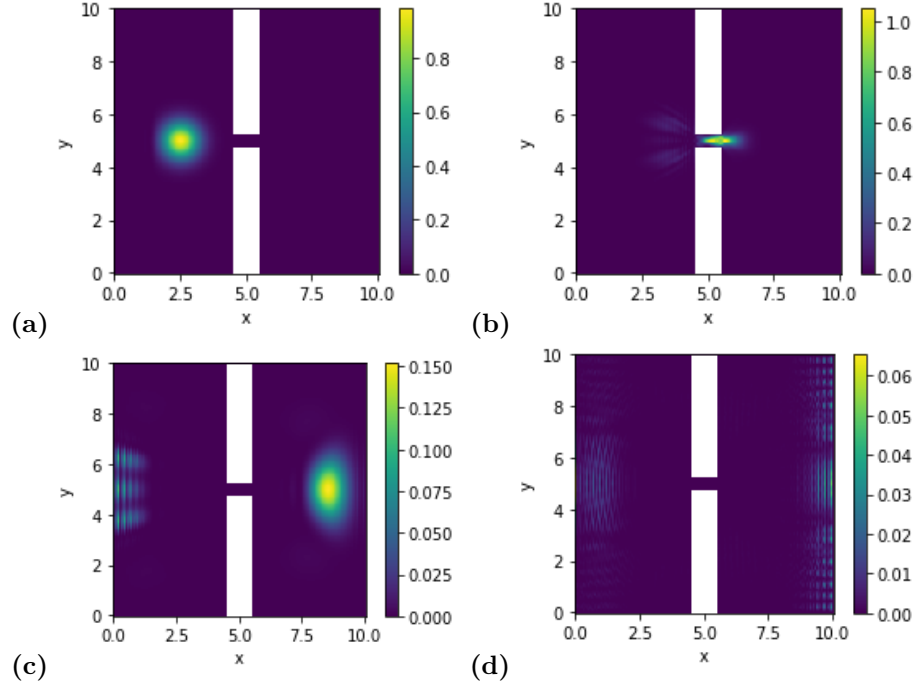


Figure 4: This figure represents the time evolution for the PDE of equation 4 using operator splitting and forcing the wave function to be zero at the slit barrier, except at the center where it can diffract. The value of  $|\Psi(t, x, y)|^2$  is being plotted, which represents a discrete probability density function. The time step is  $\Delta t = 0.005$ . The grid spacing is  $\Delta x = 0.05$ . The different plots represent the time evolution of the initial condition in equation 19 with the value of  $g = 0$ . (a)  $t = 0.1$  (b)  $t = 0.25$  (c)  $t = 0.4$  (d)  $t = 0.92$

### 5.3 Non-Linear Schrodinger equation

In equation 4, when the term  $g > 0$ , the equation 4 describes the repulsive interaction of bosons at low temperatures. This is called the defocusing case of the Non-Linear Schrodinger equation.

For the initial conditions:

$$\Psi(t = 0, x, y) = \frac{1}{5} [\sin(\frac{\pi x}{10}) \sin(\frac{\pi y}{10})] \quad (20)$$

If  $g = 0$ , this would represent a steady state solution of the linear Schrodinger equation and it would not vary over time. In this case, figure 5 uses the value of  $g = 100$  and the initial conditions are not a steady state anymore.

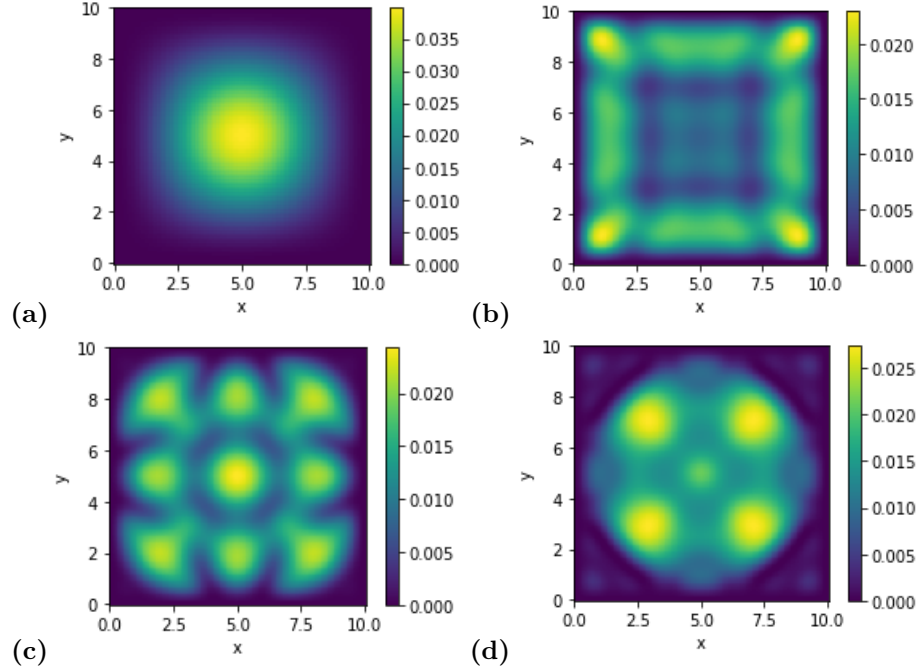


Figure 5: This figure represents the time evolution for the PDE of equation 4 using operator splitting and forcing the wave function to be zero at the boundaries. The value of  $|\Psi(t, x, y)|^2$  is being plotted, which represents a discrete probability density function. The time step is  $\Delta t = 0.025$ . The grid spacing is  $\Delta x = 0.05$ . The different plots represent the time evolution of the initial condition in equation 20 with the value of  $g = 100$ . (a)  $t = 0$  (b)  $t = 3$  (c)  $t = 6$  (d)  $t = 9$



## 6 Appendix

The code used for making these simulations can be found at [github.com/gonzalofq1/446-final](https://github.com/gonzalofq1/446-final) with documentation on how to use it.

## References

- Gross, E. P. 1961, *Nuovo Cimento*, 20, 454, doi: [10.1007/BF02731494](https://doi.org/10.1007/BF02731494)
- Seadawy, A. R. 2012, *Applied Mathematics Letters*, 25, 687, doi: <https://doi.org/10.1016/j.aml.2011.09.030>
- Zakharov, V. E., & Manakov, S. V. 1974, *Theoretical and Mathematical Physics*, 19, 551, doi: [10.1007/BF01035568](https://doi.org/10.1007/BF01035568)